

# Iridescent Chiral Nematic Cellulose Nanocrystal/Polymer Composites Assembled in Organic Solvents

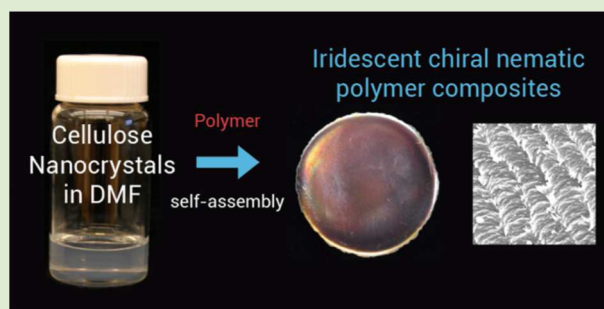
Clement C. Y. Cheung,<sup>†</sup> Michael Giese,<sup>†</sup> Joel A. Kelly,<sup>†</sup> Wadood Y. Hamad,<sup>‡</sup> and Mark J. MacLachlan<sup>\*†</sup>

<sup>†</sup>Department of Chemistry, University of British Columbia, 2036 Main Mall, Vancouver, British Columbia V6T 1Z1, Canada

<sup>‡</sup>FPIInnovations, 3800 Wesbrook Mall, Vancouver, British Columbia V6S 2L9, Canada

## S Supporting Information

**ABSTRACT:** We describe an approach to prepare polymer composites with chiral nematic photonic structures through the self-assembly of cellulose nanocrystal (CNC) dispersions in organic solvents. Contrary to previous reports, we demonstrate that dispersions of neutralized sulfated CNCs in polar organic media readily form lyotropic chiral nematic liquid crystalline phases. We have investigated the effect of the neutralizing base on the CNC self-assembly, observing chiral nematic ordering for all counterions studied. The self-assembly of the organic CNC dispersions can be exploited to prepare iridescent polymeric composites simply by casting the CNC dispersion with a suitable polymer soluble in the organic solvent. Photonic properties of the composite films can be easily controlled by either varying the ratio of CNCs to polymer or adding salts.



The discovery of cellulose nanocrystals (CNCs) prepared by acid hydrolysis of cellulose in the 1950s<sup>1,2</sup> was largely overlooked until recently,<sup>3–9</sup> when synthetic developments made them more accessible. Owing to their unique material properties, availability, biocompatibility, and nontoxicity, CNCs are of great interest for developing new materials with enhanced performance.<sup>10–16</sup> For example, CNCs have anisotropic spindle-like shapes and high surface charge (imparted by the use of strong acids such as H<sub>2</sub>SO<sub>4</sub> during hydrolysis) that cause them to form chiral nematic liquid crystalline phases at relatively low concentrations, ca. ~3–6 wt %.<sup>17,18</sup> The chiral nematic ordering can be retained in a solid film when the dispersion dries.<sup>19</sup> These films exhibit photonic properties including the selective reflection of left-handed circularly polarized light when the pitch of the chiral nematic phase is on the order of the wavelengths of visible light. The unique optical properties of solid materials with chiral nematic order have been exploited for optical applications such as sensors and filters.<sup>20,21</sup> The nanoscale dimensions and vast availability of CNCs have also attracted interest for use as a structural template.<sup>22–24</sup>

Our group has shown that the chiral nematic photonic properties of CNCs can be captured in other materials by the addition of suitable precursors that are compatible with CNC self-assembly.<sup>25–28</sup> Removal of CNCs after evaporation-induced self-assembly (EISA) by calcination or chemical extraction yields mesoporous thin films that maintain the iridescence of the chiral nematic phase. To date, this approach has been limited to precursors compatible with aqueous CNC dispersions; some materials with incompatible precursors (e.g.,

titanium) can be accessed using an alternative two-step hard templating approach.<sup>29</sup>

A straightforward method to disperse CNCs in organic media is necessary to expand the applications and processing of CNCs. Because CNCs have remarkable mechanical strength (with a Young's modulus comparable to steel), they are being widely applied to reinforce and strengthen polymer composites.<sup>30,31</sup> To achieve this goal, CNC compatibility with polymer processing is critical to ensuring homogeneous CNC dispersion within the composite.<sup>32</sup> Surface modification of CNCs has been widely studied, for example, by silylation<sup>33</sup> or grafting,<sup>34</sup> to obtain stable dispersions in organic solvents such as acetone or toluene. In some reports, the modified CNCs were shown to form chiral nematic phases, indicating surface charge is not essential for lyotropic self-assembly.<sup>35,36</sup> Heux and co-workers have shown that coating CNCs with an anionic surfactant yields colloidal dispersions in nonpolar solvents such as toluene and cyclohexane, and these form chiral nematic phases;<sup>37</sup> however, EISA of these phases into iridescent dried films was not discussed. The mesogenic properties of CNCs are strongly dependent on the cellulose feedstock, hydrolysis conditions, and ionic strength.<sup>38</sup> Surface modification introduces an additional variable that may influence chiral nematic ordering, and it can be expensive and require multiple processing steps.

Interestingly, some researchers have reported the direct dispersion of unmodified acidic CNCs (CNC-H) at ca. 0.1–1 wt % in polar organic solvents such as dimethylformamide

**Received:** September 5, 2013

**Accepted:** October 28, 2013

**Published:** November 1, 2013

(DMF), dimethylsulfoxide (DMSO), and formamide by freeze-drying aqueous dispersions followed by redispersion and extensive sonication/stirring.<sup>39,40</sup> This approach is simpler and more cost-effective than the above methods and is compatible with a wide range of commercial polymers. However, although these dispersions were shown to be strongly birefringent, no evidence for chiral nematic self-assembly was presented.

Here, we show that the neutralized form of CNCs (CNC-X, X = Li, Na, K, etc.), prepared by first treating the acidic form of CNCs (CNC-H) with an appropriate quantity of base then freeze-drying, readily disperses in polar organic media and forms chiral nematic phases through EISA to give solid films with chiral nematic photonic properties. This facile method to prepare chiral nematic phases under nonaqueous conditions significantly enhances the scope of novel photonic materials that can be prepared by CNC templating. As proof-of-concept, we demonstrate the preparation of a family of iridescent polymer composites whose optical properties can be easily tailored.

Upon neutralization of CNC-H with various strong bases and freeze-drying, we were able to easily prepare ca. 3 wt % dispersions of CNC-X (X = Li<sup>+</sup>, Na<sup>+</sup>, K<sup>+</sup>, NH<sub>4</sub><sup>+</sup>, NMe<sub>4</sub><sup>+</sup>, NBu<sub>4</sub><sup>+</sup>) in polar organic solvents including DMSO, formamide, N-methylformamide, or DMF using stirring and mild sonication (Figure 1a). The dispersions are translucent, do not precipitate out of solution, and readily pass through a 0.45 μm pore PTFE filter. In comparison, CNC-H samples handled identically are opaque white and precipitate out of solution

within minutes upon standing, indicating a poor degree of dispersibility. No significant changes in the bulk CNC composition or crystallinity after neutralization were detected by Fourier-transform infrared spectroscopy (FTIR, Supporting Information Figure S1) or powder X-ray diffraction (PXRD, Supporting Information Figure S2), consistent with this change in dispersibility arising solely through neutralizing the sulfate species.

The organic CNC-X dispersions readily form chiral nematic phases through EISA, confirmed by polarized optical microscopy (POM) during evaporation (Figure 1b, 1c and Supporting Information Figure S3). For example, POM of a CNC-Na dispersion in DMF shows the development of tactoids during evaporation, consistent with the formation of a chiral nematic phase and identical to our previous observations of aqueous CNC-H dispersions. EISA was observed for all bases we tested to neutralize the CNC-H, including alkali metal (e.g., Li<sup>+</sup>, Na<sup>+</sup>, K<sup>+</sup>) and quaternary ammonium (e.g., NH<sub>4</sub><sup>+</sup>, NMe<sub>4</sub><sup>+</sup>, NBu<sub>4</sub><sup>+</sup>) hydroxides.

Generally, we were able to disperse CNC-X in solvents capable of forming strong hydrogen bonds but not in solvents of moderate polarity such as THF. This trend is consistent with the work of Beck and co-workers, which showed that the increased H-bonding of CNC-H is a hindrance to redispersion in aqueous media.<sup>41</sup> We suggest that decreasing interparticle H-bonding by using CNC-X and employing solvents with strong solvent–particle H-bonding interactions contributes to effective dispersion. This is also consistent with previous reports that did not observe any chiral nematic organization from organic dispersions of CNC-H, as strong H-bonding interparticle interactions likely hinder formation of the chiral nematic phase.

Upon slow evaporation of the organic dispersions, we obtain iridescent thin films that give strong signals with positive ellipticity when analyzed by circular dichroism (CD) spectroscopy. These signals are consistent with the selective reflection of left-handed circularly polarized light from a chiral nematic structure (Supporting Information Figures S4 and S5). We obtained iridescent thin films from a range of polar organic solvents, but we primarily worked with DMF dispersions due to its lower boiling point, which gives shorter evaporation times.

Scanning electron microscopy (SEM) of a cross-section of a dried CNC-Na film cast from DMF shows a helical layered structure normal to the film's surface (Figure 1d and Supporting Information Figure S6), with a repeat distance on the order of the wavelengths of visible light. This is consistent with the Bragg-like reflection of light from chiral nematic liquid crystals, governed by the relation

$$\lambda = n_{\text{avg}} P \sin \theta$$

where  $n_{\text{avg}}$  is the average refractive index (ca. 1.54 for crystalline cellulose);  $P$  is the repeat distance of the helical pitch; and  $\theta$  is the angle of incidence. UV–vis spectroscopy of the CNC-X films (Supporting Information Figures S7 and S8) shows a blue shift in the reflected color with increasing size of the alkali metal cations and a red shift with increasing hydrophobicity for the alkylammonium cations, consistent with previous studies of aqueous CNC-X indicating the interplay between cation size and hydrophobicity in influencing the chiral self-assembly of CNCs.<sup>37</sup> We also observed that the initial CNC-X concentration influences the resulting reflected color, similar to previous studies on aqueous CNC-H (Supporting Information Figure S9).<sup>42</sup>

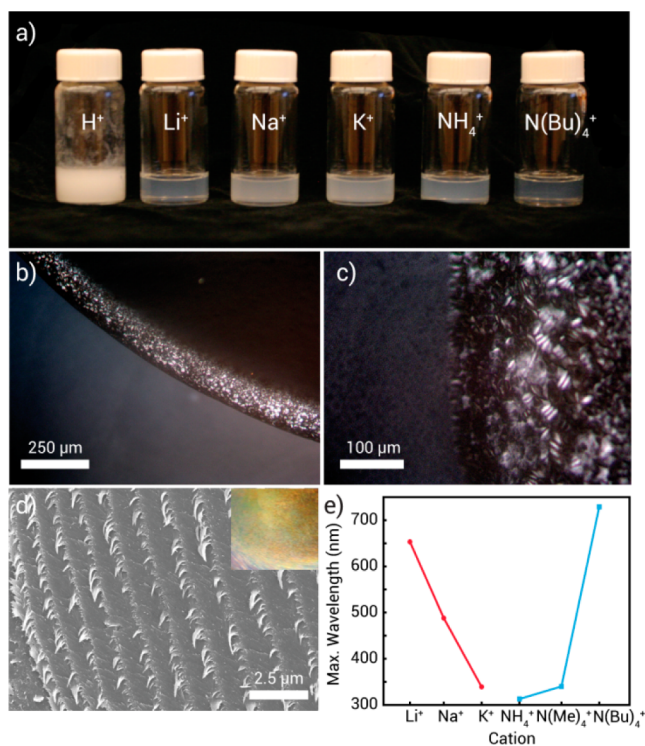


**Figure 1.** (a) Visual comparison of 3 wt % DMF suspensions of CNC-X. (b) and (c) POM images of 3% CNC-NH<sub>4</sub> and CNC-Li dispersions in DMF showing the formation of spherulite-like structures during evaporation. (d) SEM of a cross-section of a dried CNC-Na film (inset: photograph of the iridescent film). (e) The maximum reflected wavelength measured by CD spectroscopy from dried CNC-X films as a function of cation.

Thermogravimetric analysis (TGA) of the CNC-X revealed that cation-exchanged CNCs are generally more thermally stable than CNC-H, where alkali metals have the most pronounced improvement to the degradation temperature (Supporting Information Figure S10).

A variety of materials whose precursors are incompatible with acidic aqueous CNC-H dispersions can be accessed by switching to polar organic solvents. For example, many commodity polymers, such as polystyrene (PS), poly(methyl methacrylate) (PMMA), polycarbonate (PC), and poly(9-vinylcarbazole) (PVK), are soluble in DMF. Mixing these polymers with CNC-Na dispersions (3.5 wt %) in DMF followed by slow evaporation of the solvent is a facile way to prepare iridescent composite films with chiral nematic structure (Figure 2a). We were also able to prepare polymer composites with other CNC-X cations but present our results here with CNC-Na for consistency.

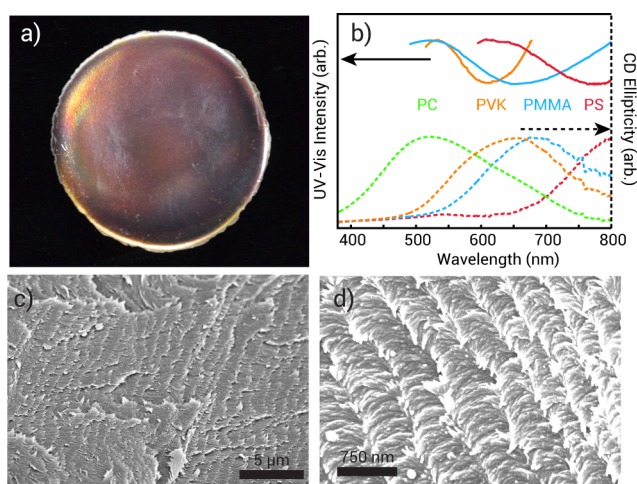


**Figure 2.** (a) Photograph of an iridescent CNC-Na/PMMA composite film with chiral nematic ordering. (b) UV-vis and CD spectra of composites with 46 wt % polymer prepared with PS, PMMA, PC, and PVK (UV-vis spectrum of CNC-Na/PC is omitted because of strong absorption of the polymer around the reflected wavelength). (c) Representative SEM image of a CNC-Na/PC composite demonstrating the periodic layered structure. (d) At higher magnification, SEM shows the left-handed helical morphology of the spindle-shaped CNCs.

Understanding the effect of water absorption by the dispersion during EISA was crucial to the successful preparation of these composites. Films cast under ambient conditions were cloudy white due to precipitation of the polymer. The films exhibited an inhomogeneous morphology with an opaque white base containing the polymer and a slightly iridescent upper layer containing the CNCs (Supporting Information Figure S11). As the initial mixture of CNC-Na and polymer in the polar organic solvents appeared homogeneous, we thought that the slow evaporation rates and hygroscopic nature of the solvents caused them to absorb water during EISA, which in turn led to phase separation. Indeed, carrying out EISA under a flow of dry air yields iridescent, homogeneous composite films with excellent optical clarity. We characterized the chiral nematic composite films by TGA, differential scanning calorimetry (DSC), POM, PXRD, SEM, and CD spectroscopy. TGA indicates that the composites are stable to 265–275 °C, with onsets of decomposition ~25–35 °C lower than the

CNC-Na itself (Supporting Information Figure S12 and Table S1). DSC analysis of the polymer composites (54 wt % CNC-Na) showed substantial broadening of the glass transition temperature such that it could not even be seen in some cases (Supporting Information Figure S13). Annealing of the composites at 200 °C for 30 min prior to the DSC analysis did not improve the observation of a  $T_g$ . This broadening is often observed in the case of polymer composites with a high loading of a nanoscale additive and is attributed to surface interactions between CNCs and the polymer.<sup>43</sup>

The composite films are visibly iridescent. POM images show strong birefringence and a texture characteristic of chiral nematic ordering (Supporting Information Figure S14). All composites showed strong positive CD signals that correspond to the reflected color measured by UV-vis spectroscopy (Figure 2b). At a constant polymer loading of 46 wt %, the reflected color from the composites shifts depending on the polymer used. The light reflected ranges across the visible spectrum from ca. 800 nm for PS composites down to ca. 500 nm for PC composites, suggesting polymer hydrophobicity modulates CNC EISA. PC and PVK strongly absorb in the UV; while we expect a CD signal (Cotton effect) associated from the chiral organization of these absorbing species as we observed for nanoparticles inside chiral nematic structures,<sup>44</sup> it is likely the reflection associated with the chiral nematic order that overwhelms this signal. SEM images taken throughout the thickness of the film and from multiple regions clearly show a homogeneous, twisting layered motif for all investigated polymer composites, matching the morphology observed for pure CNC-X films (Figure 2c, 2d and Supporting Information Figure S15). Overall, the crystallinity of the CNCs remained unaffected by the presence of polymer (PXRD, Supporting Information Figure S16).

Increasing the polymer/CNC-Na ratio gives a gradual red shift in the reflected color of the iridescent composites due to an increasing helical pitch, offering a simple method to control the optical properties and further supporting the intimate mixing of the CNCs and polymer within the chiral nematic structure. For example, increasing the PS loading in CNC-Na/PS composites from 36 to 59 wt % leads to a red shift from ca. 700 nm up to 1135 nm in the reflection maximum (Figure 3a).

At very high PS loading (e.g., 70 wt %), no reflected color is observed by UV-vis spectroscopy, consistent with disruption of the chiral nematic phase. However, SEM of these composites shows a layered, nematic-like morphology indicative of lyotropic CNC organization even at these low concentrations (Supporting Information Figure S17).

The chiral nematic organization of these composites indicates excellent dispersal of the CNC-Na throughout the polymer matrix. This is an important criterion for the use of CNCs as a reinforcing agent in polymer composites. Although not our primary goal in preparing these composite materials, we are currently investigating the mechanical properties of these composites to compare to other reports of CNC-reinforced polymer composites.<sup>30,31</sup>

For films cast from aqueous dispersions of CNCs, the addition of salts results in a blue shift of the reflected color.<sup>38</sup> We observe a similar effect for the CNC-X dispersions in organic solvents by adding LiCl, a DMF-soluble salt, to a CNC-Na/PS dispersion before EISA (Figure 3b). A gradual blue shift in the reflected color of the samples is observed; high LiCl loadings lead to a loss of color, presumably due to the

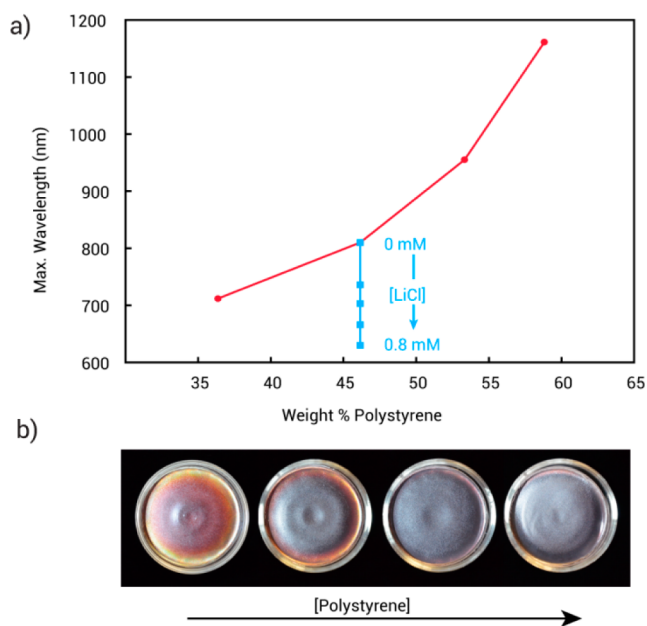


**Figure 3.** (a) Maximum reflected wavelength measured by UV–vis spectroscopy as a function of PS content and ionic strength. (b) Photograph of CNC-Na/PS composite films showing the red shift in color with increasing polymer to CNC-Na ratio.

disruption of chiral nematic ordering, where no fingerprint texture was observed under POM.

In light of the extensive work that has been undertaken to compatibilize CNCs for nanocomposite preparation, we were surprised that our simple method leads to very homogeneous photonic films. Even highly hydrophobic polymers, such as PS, are homogeneously distributed within the chiral nematic matrix of CNC-Na, a hydrophilic material. One would expect phase separation due to the poor interactions between the components, but this does not occur. This new approach may be useful for preparing diverse materials with chiral nematic order.

In conclusion, we have developed a straightforward method to generate new iridescent polymer composites with chiral nematic structures by successfully dispersing neutralized CNC in polar organic solvents such as DMF. This approach is easily scalable to obtain large area thin films and coatings that could be used for applications such as reflective filters. We expect the general method of using organic dispersions of CNC as a chiral nematic template may lead to a broad variety of new photonic composite or mesoporous materials.

## ■ ASSOCIATED CONTENT

### Supporting Information

Experimental procedures, POM, UV–vis, CD, SEM, FTIR, PXRD, DSC, and TGA. This material is available free of charge via the Internet at <http://pubs.acs.org>.

## ■ AUTHOR INFORMATION

### Corresponding Author

\*E-mail: [mmaclach@chem.ubc.ca](mailto:mmaclach@chem.ubc.ca). Fax: (604) 822-2847. Tel.: (604) 822-3070.

### Notes

The authors declare no competing financial interest.

## ■ ACKNOWLEDGMENTS

We thank the Natural Sciences and Engineering Research Council (NSERC) for funding and FPInnovations for CNCs. MG and JAK are grateful to the German Academic Exchange Service (DAAD) and NSERC, respectively, for postdoctoral fellowships. We thank Spencer Serin for GPC analyses.

## ■ REFERENCES

- (1) Rånby, B. G. *Discuss. Faraday Soc.* **1951**, *11*, 158–164.
- (2) Mukherjee, S. M.; Sikorski, J.; Woods, H. J. *J. Text. Inst.* **1952**, *43*, T196–T201.
- (3) Klemm, D.; Kramer, F.; Moritz, S.; Lindstrom, T.; Ankerfors, M.; Gray, D.; Dorris, A. *Angew. Chem., Int. Ed.* **2011**, *50*, 5438–5466.
- (4) Habibi, Y.; Lucia, L. A.; Rojas, O. J. *Chem. Rev.* **2010**, *110*, 3479–3500.
- (5) Samir, M. A. S. A.; Alloin, F.; Dufresne, A. *Biomacromolecules* **2005**, *6*, 612–626.
- (6) Hubbe, M. A.; Rojas, O. J.; Lucia, L. A.; Sain, M. *Bioresources* **2008**, *3*, 929–980.
- (7) Siqueira, G.; Bras, J.; Dufresne, A. *Polymers* **2010**, *2*, 728–765.
- (8) Moon, R. J.; Martini, A.; Nairn, J.; Simonsen, J.; Youngblood, J. *Chem. Soc. Rev.* **2011**, *40*, 3941–3994.
- (9) Lin, N.; Huang, J.; Dufresne, A. *Nanoscale* **2012**, *4*, 3274–3294.
- (10) Hasani, M.; Cranston, E. D.; Westman, G.; Gray, D. G. *Soft Matter* **2008**, *4*, 2238–2244.
- (11) Padalkar, S.; Capadona, J. R.; Rowan, S. J.; Weder, C.; Won, Y.-H.; Stanciu, L. A.; Moon, R. J. *Langmuir* **2010**, *26*, 8497–8502.
- (12) Fox, J.; Wie, J. J.; Greenland, B. W.; Burattini, S.; Hayes, W.; Colquhoun, H. M.; Mackay, M. E.; Rowan, S. J. *J. Am. Chem. Soc.* **2012**, *134*, 5362–5368.
- (13) Way, A. E.; Hsu, L.; Shanmuganathan, K.; Weder, C.; Rowan, S. J. *ACS Macro Lett.* **2012**, *1*, 1001–1006.
- (14) Lin, N.; Dufresne, A. *Biomacromolecules* **2013**, *14*, 871–880.
- (15) Biyani, M. V.; Foster, E. J.; Weder, C. *ACS Macro Lett.* **2013**, *2*, 236–240.
- (16) Jin, H.; Kettunen, M.; Laiho, A.; Pynnonen, H.; Paltakari, J.; Marmur, A.; Ikkala, O.; Ras, R. H. A. *Langmuir* **2011**, *27*, 1930–1934.
- (17) Marchessault, R. H.; Morehead, F. F.; Walter, N. M. *Nature* **1959**, *184*, 632–633.
- (18) Revol, J. F.; Godbout, L.; Gray, D. G. *J. Pulp. Pap. Sci.* **1998**, *24*, 146–149.
- (19) Revol, J.-F.; Bradford, H.; Giasson, J.; Gray, D. G. *Int. J. Biol. Macromol.* **1992**, *14*, 170–172.
- (20) Herzer, N.; Guneyssu, H.; Davies, D. J. D.; Yildirim, D.; Vaccaro, A. R.; Broer, D. J.; Bastiaansen, C. W. M.; Schenning, A. P. H. J. *J. Am. Chem. Soc.* **2012**, *134*, 7608–7611.
- (21) Zhang, Y. P.; Chodavarapu, V. P.; Kirk, A. G.; Andrews, M. P. *Sens. Actuators, B: Chem.* **2013**, *176*, 692–697.
- (22) Kloser, E.; Gray, D. G. *Langmuir* **2010**, *26*, 13450–13456.
- (23) Dujardin, E.; Blaseby, M.; Mann, S. *J. Mater. Chem.* **2003**, *13*, 696–699.
- (24) Shin, Y.; Exarhos, G. J. *Mater. Lett.* **2007**, *61*, 2594–2597.
- (25) Shopsowitz, K. E.; Qi, H.; Hamad, W. Y.; MacLachlan, M. J. *Nature* **2010**, *468*, 422–425.
- (26) Shopsowitz, K. E.; Hamad, W. Y.; MacLachlan, M. J. *J. Am. Chem. Soc.* **2012**, *134*, 867–870.
- (27) Kelly, J. A.; Shukaliak, A. M.; Cheung, C. C. Y.; Shopsowitz, K. E.; Hamad, W. Y.; MacLachlan, M. J. *Angew. Chem., Int. Ed.* **2013**, *52*, 8912–8916.
- (28) Khan, M. K.; Giese, M.; Yu, M.; Kelly, J. A.; Hamad, W. Y.; MacLachlan, M. J. *Angew. Chem., Int. Ed.* **2013**, *52*, 8921–8924.
- (29) Shopsowitz, K. E.; Stahl, A.; Hamad, W. Y.; MacLachlan, M. J. *Angew. Chem., Int. Ed.* **2012**, *51*, 6886–6890.
- (30) Cao, X.; Dong, H.; Li, C. M. *Biomacromolecules* **2007**, *8*, 899–904.
- (31) George, J.; Ramana, K. V.; Bawa, A. S.; Siddaramaiah. *Int. J. Biol. Macromol.* **2011**, *48*, 50–57.

- (32) Mohanty, A. K.; Misra, M.; Drzal, L. T. *Compos. Interfaces* **2001**, *8*, 313–343.
- (33) Grunert, M.; Winter, W. T. *J. Poly. Environ.* **2002**, *10*, 27–30.
- (34) Araki, J.; Wada, M.; Kuga, S. *Langmuir* **2001**, *17*, 21–27.
- (35) Yi, J.; Xu, Q.; Zhang, X.; Zhang, H. *Polymer* **2008**, *49*, 4406–4412.
- (36) Elazzouzi-Hafraoui, S.; Putaux, J.-L.; Heux, L. *J. Phys. Chem. B* **2009**, *113*, 11069–11075.
- (37) Heux, L.; Chauve, G.; Bonini, C. *Langmuir* **2000**, *16*, 8210–8212.
- (38) Dong, X. M.; Kimura, T.; Revol, J. F.; Gray, D. G. *Langmuir* **1996**, *12*, 2076–2082.
- (39) Viet, D.; Beck-Candanedo, S.; Gray, D. G. *Cellulose* **2007**, *14*, 109–113.
- (40) Tang, L.; Weder, C. *ACS Appl. Mater. Interfaces* **2010**, *2*, 1073–1080.
- (41) Beck, S.; Bouchard, J.; Berry, R. *Biomacromolecules* **2012**, *13*, 1486–1494.
- (42) Pan, J.; Hamad, W.; Straus, S. K. *Macromolecules* **2010**, *43*, 3851–3858.
- (43) Miaudet, P.; Derre, A.; Maugey, M.; Zakri, C.; Piccione, P. M.; Inoubli, R.; Poulin, P. *Science* **2007**, *318*, 1294–1296.
- (44) Qi, H.; Shopsowitz, K. E.; Hamad, W. Y.; MacLachlan, M. J. *J. Am. Chem. Soc.* **2011**, *133*, 3728–3731.